A Closed-loop Inductive Power Control System for an Instrumented Strain Sensing Tibial Implant

Shiying Hao, *IEEE Member*, and Stephen Taylor, *IEEE Member*

***Abstract*— Inductively-powered implantable biomedical devices are widely used nowadays, however the power variations due to the coil misalignment can significantly affect the device performance. A closed-loop power control system is proposed in this paper, which is implemented in a Subject-Carried Implant Monitoring Inductive Telemetric Ambulatory Reader (SCIMITAR) for remote strain data acquisition from an instrumented ovine tibia implant. The output power of the energizer is adaptively adjusted via a feedback circuitry connected the demodulator with the power energizer. Lab results showed that feedback suppressed variations in induced power caused by coil misalignment and extended the functional range of the device in axial and planar directions.**

I. Introduction

Forces and moments exerted on bone fracture supporting implants during daily activities are the main indicators of bone healing status [1-2]. To enable strain measurements in vivo under load after surgery, a few instrumented implants have been developed [2-4] to record strain data. An inductive telemetry link was always used to establish data, power and command communication between the implanted device and the external device [5-6].

Since the telemetry link is the critical part to communicate between the implanted and the external system in biomedical applications, many studies were concentrated on the optimization of its power transmission efficiency [5-14]. Among these methods, the closed-loop design is popular, due to its small size and low cost. So far closed-loop power control systems have been reported in applications of many implants [12-14]. However, there are no reports yet of a closed-loop system in applications of bone implants.

A closed-loop Subject-Carried Implant Monitoring Inductive Telemetric Ambulatory Reader (SCIMITAR) [15] for strain, voltage and temperature data acquisition from an instrumented ovine nail implant is proposed in this paper. The aim of the device is to remotely monitor the healing status of the ovine tibia bone fracture over months. It consist of three parts: an implanted sensor to record data, an external power energizer and data demodulator, and an inductive link for power and data transmission. A closed-loop power control scheme is applied between the energizer and the demodulator, so as to adaptively adjust the output power of the energizer based on the amplitude of the demodulated signals. The feedback effectively suppresses the impact of the coil misalignment on the device functional ranges in both axial and planar directions. Measured results in the lab show that the flexibility and reliability of the whole system are both improved by using the closed-loop scheme. To our knowledge, it is the first closed-loop data acquisition device that is implemented on artificial orthopaedic implants.

Research supported by Technology Strategy Board and Smith & Nephew.

Shiying Hao is with the School of Medicine, Stanford University, CA 94305 USA (corresponding author to provide phone: 517-331-1846; e-mail: zxrlwj@ gmail.com).

Stephen Taylor is with the Institute of Orthopaedics and Musculoskeletal Science, University College London, HA7 4LP, UK (e-mail: stephen.taylor@ucl.ac.uk).

II. Materials and Methods

A. System Configurations

The SCIMITAR (Fig 1) consists of three main parts: an instrumented implant, an external energizer and demodulator and a telemetry link. The feedback module is implemented between the energizer and the demodulator.

Fig 2 is a picture of a 18cm long×10mm outer diameter×4.7mm inner diameter TRIGEN META TIBIAL NAIL. It has two pockets on the anterior face. One is the telemetry pocket ($18\times5.4\times3.1mm^3$) with a coil placed in it to receive power and send data. The other is the circuitry pocket ($40\times6.5\times3mm^3$) where a flexible PCB is mounted, with strain gauges attached underneath. The strain data integrated with temperature & voltage data are converted to digital signals, then load-shift-keying (LSK) modulated and sent to the external demodulator via a pair of coils. The implanted electronic circuitry is powered inductively from the external energizer.

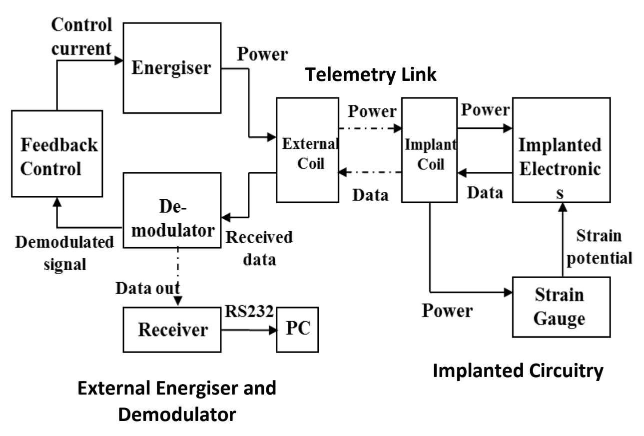

Fig 1. The block diagram of the whole system. Dashed lines represent wireless link

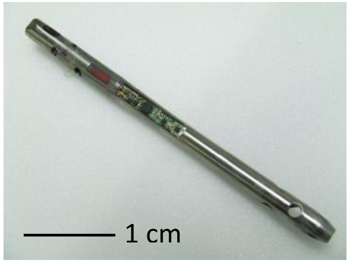

Fig 2. An instrumented nail implant, with a telemeter coil and a flexible PCB mounted on the pockets. The strain gauges are attached underneath the PCB.

Fig 3 is the block diagram of the external module, including a power energizer to power the implanted electronics and a demodulator to pick up strain information and to send to PC for analysis. A feedback module connects the two blocks together, forming a closed-loop system. The energizer includes a battery, a step-down DC-DC converter and a class D power amplifier. The output power level is either manually controlled by a remote infrared controlled digital potentiometer (EPOT in Fig 3) or automatically controlled by a feedback circuitry.

The bidirectional telemetry is constructed by a pair of inductive coils. They are both single layer and cylindrical due to the constraints of the space available. The implanted coil has 50 turns, winded on a ferrite (12.5mm×3.3mm×1.5mm) using 0.2mm copper wire. The external coil has 40 turns, 110mm diameter, wound using 16/0.2mm copper wire. The operating tuned frequency is 152kHz.

B. System Performance Indicators

The performance of the remotely controlled instrumented implant can be evaluated by the maximum allowable coil misalignment in the axial and planar directions, within which the sufficient power delivered to the implant and the accuracy of the reconstructed data at the demodulator can be maintained. The minimum power needed to operate the implant load is 32mW. The maximum acceptable error is 0.5 bit in the reconstructed data. If there was any more than 0.5 bit error between the original data and reconstructed data, the synchronization between the receiver and PC would be lost.

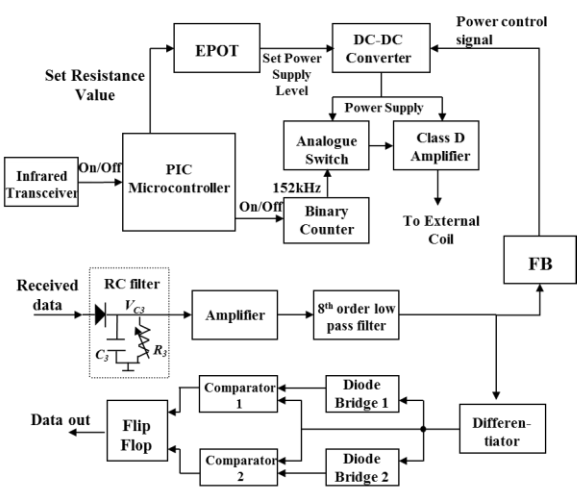

Fig 3. The block diagram of the external power energizer and signal demodulator. A feedback circuitry (FB) converts demodulated signal into control signal to adjust the power supply level.

Whether or not the two coils are well coupled is a critical condition to maintain a functional system. Insufficient power due to loose coupling may stop the implanted circuitry working, whilst too much power will cause signal clamping and reduce the data reconstruction accuracy. Preliminary tests showed that the pulse width error of the reconstructed data increases by 30% with planar misalignment up to 30mm. As a result, a feedback scheme is needed to suppress such misalignment effects, in order to maximize the misalignment tolerance in both axial and planar directions, and therefore to improve the system performance.

C. Feedback Scheme

Fig 4 is the schematic of the feedback circuitry. It is composed of two peak detectors, an instrumented differential amplifier, a voltage divider and a current control resistor. The output signal of the low pass filter in the demodulator goes through two detectors where its absolute amplitude is extracted and amplified in the following amplifier. The amplified DC signal is divided by a pair of potentiometers and sent to the reference pin of a commercial step-down DC-DC converter via a control resistor R_C. R_C converts the DC voltage signal V_i into a current signal I_C. Because the output signal V_{DC} (i.e. the power supply of the class D power amplifier) of the DC converter is controlled by $R_{5,6}$, I_C and V_r, and $R_{5,6}$ and V_r are all constant, the value of V_{DC} depends on I_C and thus the amplitude of the received signal at the filter output (V_a). The feedback algorithm is presented as below.

The expression of I_C is:

$$I_C = \frac{V_a \cdot \frac{R_4}{R_3 + R_4} - V_{FB}}{R_C} \tag{1}$$

The DC power supply V_{DC} is:

$$V_{DC} = V_{FB} + R_5 \cdot \left(\frac{V_{FB}}{(R_6 + R_{EPOT})//R_8} - I_C - \frac{V_r - V_{FB}}{R_7} \right) \tag{2}$$

The power transmitted into the implant can be written as:

$$P_{im} = V_{DC} I_{DC} \cdot \frac{k^2}{k^2 + k_{crit}^2} \approx \frac{V_{DC}^2}{R_S} \cdot \frac{k^2}{k^2 + k_{crit}^2} \tag{3}$$

where k_{crit} is the critical coupling coefficient of the inductive link, I_{DC} is the DC current on the external coil.

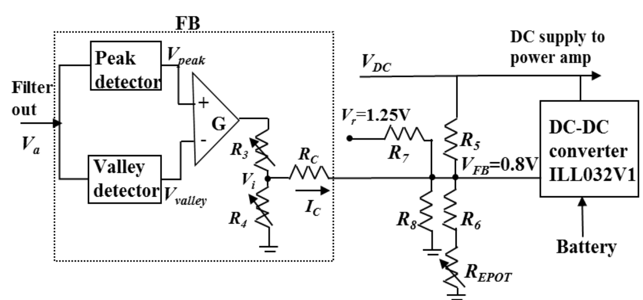

Fig 4. The schematic of the feedback (FB) circuitry. The input of FB is the output signal of the LPF as shown in Fig 3. The output of FB is a current control signal IC controlling the DC supply of the power amplifier (V_{DC}) via a DC-DC converter. V_r is a constant 1.25V reference voltage. V_{FB} is connected to the feedback pin of the DC-DC converter. R_{EPOT} is the resistance of a potentiometer digitally controlled by an infrared device.

According to Fig 3 & 5 and the Appendix, V_a can be written as:

$$V_a \approx A \cdot |H_f| \cdot k^2 \cdot \frac{V_{DC}}{2\omega C_F} \cdot \frac{C_2}{C_1} \cdot \frac{\Delta R_2}{R_1^2} \tag{4}$$

By substituting eqn (1), (2), (4) to (3), the relationship between P_{im} and k can be expressed as:

$$P_{im} = \frac{1}{R_S} \cdot \left[\left(1 + \frac{R_5}{(R_6 + R_{EPOT})//R_8} + \frac{R_5}{R_C} + \frac{R_5}{R_7}\right) \cdot V_{FB} - \frac{R_5 \cdot V_r}{R_7} - Uk^2\right]^2 \cdot \frac{k^2}{(k^2 + k_{crit}^2)} \tag{5}$$

where

$$U \approx A \cdot |H_f| \cdot \frac{1}{2\omega C_F} \cdot \frac{C_2}{C_1} \cdot \frac{\Delta R_2}{R_1^2} \cdot \frac{R_4}{R_3 + R_4} \cdot \frac{R_5}{R_C}$$

When there is no feedback, U=0. Eqn (5) indicates the variations in P_{im} caused by k can be reduced by the existence of Uk^2. Hence the use of feedback can compensate the effect of the coil misalignment on P_{im} and extend the functional ranges of the implanted device in planar and axial directions.

An advantage of this feedback design is that V_{DC} is adjusted by measuring the signal amplitude V_a at the receiver side. There is no need to send any information of implant power via the wireless link to accomplish the feedback control like other studies [10-14], which reduces the data bandwidth requirement.

I. System Implementation

An instrumented tibia implant as shown in Fig 2 was used for experiments on bench. The properties of the implant and the external coils are listed in Table 1. The external energizer, demodulator and feedback circuitry were fabricated on 3 PCBs. In all experiments, the resistance values of the feedback circuit shown in Fig 4 were set as follows: R_3=12.87kΩ, R_4=6.77kΩ, R_5=300kΩ, R_6=40kΩ, R_7=4.7kΩ, R_8=6.8kΩ, R_C=55kΩ, R_{EPOT} ranges from 0 to 100kΩ.

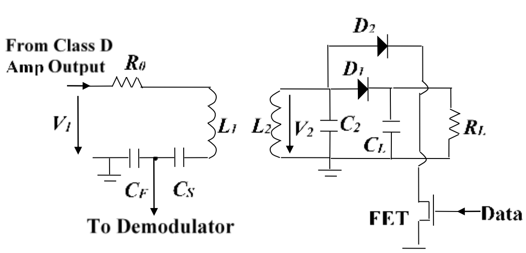

(a)

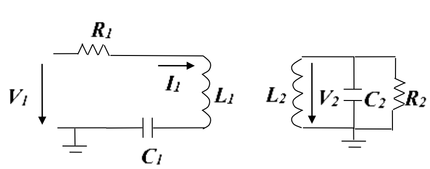

(b)

Fig 5. a) Circuit diagram of the inductive link. L_1, L_2 are external and implant coils. C_2, C_F, C_S are tuning capacitors. R_0 is the output resistance of the energizer. R_L is the equivalent resistance of the load circuit; b) Equivalent circuit diagram (a). $R_{1,2}$ are the total equivalent resistance of the primary and secondary circuits.

TABLE 1. PROPERTIES OF COILS WITH CARRIER FREQUENCY OF 152 KHZ.

Properties	External Coil	Internal Coil
Wire	16/0.2mm copper	0.2mm diameter copper
Number of layers	1	1
Dimension	110mm OD	3.5×12.5×1.5mm^3
Inductance	227.7μH	21.8μH
Tuning capacitance	4.68nF	52.8nF
self-resistance	1.97Ω	100 Ω
Number of turns	40	50
Q	110	4.8
Critical coupling coefficient	0.0518	
Load resistance	R_2 = 65 Ω, R_L = 500 Ω, R_{FET}+R_{D2}= 750 Ω	

The implant power and the reconstructed data accuracy were both observed on GUI to work out the maximum allowable coil misalignment and to evaluate the feedback performance. The axial maximum allowable coil misalignment was determined by where the implant power reduced to 32mW. The planar maximum allowable misalignment was determined by where the data became undetectable, i.e. the PC program lost synchronization.

II. Results

Fig 6(a) - (b) show the implanted power P_{im} with respect to the planar and axial coil misalignment, with different values of EPOT. It is clear that the P_{im} variations measured with the use of the feedback circuit are smaller than those measured without feedback. Table 2 illustrates the functional ranges of the device in planar and axial directions, i.e. the coil misalignment ranges within which 1) the P_{im} is sufficient (>32mW) and 2) the received data are reconstructed accurately so that they can be detected by the PC-based program. Data in Table 2 show that the functional ranges measured with the use of the feedback are larger than those obtained without feedback, in both planar and axial directions. Results in Fig 6 and Table 2 verify that the feedback circuit can suppress the P_{im} variations and extend the functional ranges in spite of coil misalignment.

It should be noted that P_{im} variations caused by the coil misalignment can't be eliminated by the feedback, i.e. the increase of V_{DC}, because 1) the decrease of k with the misalignment is too rapid to be compensated, and 2) V_{DC} has an upper limit of 16V. Therefore the feedback can slow down the variations of P_{im}, but can't eliminate it.

III. Conclusion

A closed-loop power control scheme is developed in this paper, which is implemented in our custom-made SCIMITAR system for remote data acquisition from orthopaedic implants. It is able to suppress the implanted power variations by feeding back the demodulated signal into the power energizer to achieve the automatic adjustment. Comparing to the open-loop system, the closed-loop design has the advantage that the functional ranges of the device, within which the demodulated data are reconstructed accurately with sufficient implanted power, are larger in both planar and axial

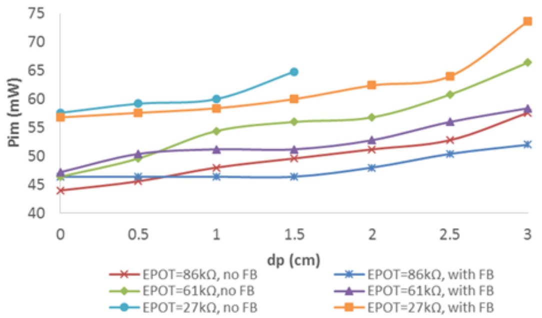

(a)

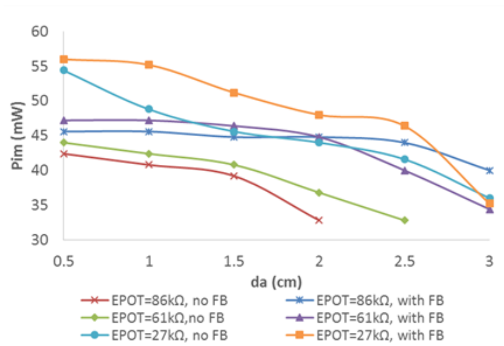

(b)

Fig 6. The implanted power P_{im} as a function of the (a) planar and (b) axial coil misalignment (*dp* and *da*), with or without feedback system applied. *da* and *dp* are horizontal and vertical distances between two coils. It was measured with different EPOT settings, giving different V_{DC}.

TABLE 2. THE FUNCTIONAL RANGES OF THE DEVICE (I.E. THE MAXIMUM ALLOWABLE COIL MISALIGNMENT) IN AXIAL AND PLANAR DIRECTIONS.

R_{EPOT} (kΩ)	Axial (cm)		Planar (cm)	
	With feedback	Without feedback	With feedback	Without feedback
86	±3.3	±2	±4	±4
61	±3.3	±2.5	±4	±4
27	±3.3	±3.3	±3	±1.5

directions. To our knowledge, it is the first closed-loop, remote data acquisition device used on instrumented orthopaedic implants.

APPENDIX

In Fig 2, the variations in R_2 due to the modulation are reflected to R_{1TOT} (the total resistance on the primary stage) and modulate the voltage across C_F. Assume $|V_{FH}|$ and $|V_{FL}|$ represent the RMS voltage across C_F when data is high and low respectively:

$$|V_{F_H}| = \frac{|I_{F_H}|}{\omega C_F} = \frac{|V_{DC_{RMS}}|}{\omega C_F R_{1TOT_H}} = \frac{|V_{DC_{RMS}}|}{\omega C_F (R_1 + k^2 \frac{C_2}{C_1} R_{2H})}$$

$$|V_{F_L}| = \frac{|I_{F_L}|}{\omega C_F} = \frac{|V_{DC_{RMS}}|}{\omega C_F R_{1TOT_L}} = \frac{|V_{DC_{RMS}}|}{\omega C_F (R_1 + k^2 \frac{C_2}{C_1} R_{2L})} \qquad (A.1)$$

where $|I_{FH}|$ and $|I_{FL}|$ are RMS current through C_F, $|R_{1TOTH}|$ and $|R_{1TOL}|$ are $|R_{1TOT}|$ during high and low data output. $|V_{DCRMS}|$ is the RMS supply of the power amplifier.

The voltage at the filter output (V_a) can be expressed as:

$$|V_a| = |H_f| \cdot (|V_{F_H}| - |V_{F_L}|)$$

$$= |H_f| \cdot k^2 \cdot \frac{V_{DC_{RMS}}}{\omega C_F} \cdot \frac{C_2}{C_1} \cdot \frac{R_{2L} - R_{2H}}{(R_1 + k^2 \frac{C_2}{C_1} R_{2H})(R_1 + k^2 \frac{C_2}{C_1} R_{2L})}$$

$$\approx k^2 \cdot \frac{V_{DC}}{2\omega C_F} \cdot \frac{C_2}{C_1} \cdot \frac{R_{2L} - R_{2H}}{R_1^2} \qquad (A.2)$$

ACKNOWLEDGMENT

The support of the Technology Strategy Board and Smith & Nephew, are gratefully acknowledged.

REFERENCES

[1] Wilson D.J., et al., A single-channel telemetric intramedullary nail for in vivo measurement of fracture healing. Journal of Orthopaedic: Trauma. 2009, 23(10): pp.702-709.

[2] Schneider E. et al., Loads acting in an intramedullary nail during fracture healing in the human femur. J. Biomech. 2001, 34(7): pp.849-857.

[3] Elfström G., Nachemson A., Telemetry recordings of forces in the Harrington distraction rod: a method for increasing safety in the operative treatment of scoliosis patients. Clin. Orthop. Relat. Res. 1973, 93: pp.158-172.

[4] Faroug R. et al., Strain response of an instrumented intramedullary nail to three-point bending. Journal of Medical Engineering & Technology. 2011, 35 (5): pp.275-282.

[5] Taylor S., et al. Telemetry of forces from proximal femoral replacements and relevance to fixation, Journal of Biomechanics, 1997, 30(3): pp.225-234.

[6] Taylor S., Walker P.S., Forces and moments telemetered from two distal femoral replacements during various activities, Journal of Biomechanics, 2001, 34(7): pp.839-848.

[7] Geisler M.S., Jeutter D.C., An implantable transcutaneously programmable and rechargeable nerve regenerator with telemetry links. Engineering in Medicine and Biology Society, 1993. Proceedings of the 15th Annual International Conference of the IEEE. 1993, pp.1240-1241.

[8] Ackermann D.M. et al., Designing the optical interface of a transcutaneous optical telemetry link. Biomedical Engineering, IEEE Transactions on. 2008, 55(4): pp.1365-1373.

[9] RamRakhyani A.K., Lazzi G., On the design of efficient multi-coil telemetry system for biomedical implants. Biomedical Circuits and Systems, IEEE Transactions on. 2013, 7(1): pp.11-23.

[10] David C Ng, et al., Wireless technologies for closed-loop retinal prostheses. J Neural Eng. 2009, 6(6): 065004.

[11] Guoxing Wang., et al., Design and analysis of an adaptive transcutaneous power telemetry for biomedical implants. Circuits and Systems I: Regular Papers, IEEE Transactions on. 2005, 52(10): pp.2109-2117.

[12] Hongcheng Xu, et al., A multichannel neurostimulator with transcutaneous closed-loop power control and self-adaptive supply. ESSCIRC, 2012 Proceedings of the. 17-21 Sept. 2012: pp.309-312.

[13] Silay K.M., Dehollaini C., Declercq M., Inductive power link for a wireless cortical implant with two-body packaging. Sensors Journal, IEEE. 2011, 11(11): pp.2825-2833.

[14] Kiani M. et al., Evaluation of a closed loop inductive power transmission system on an awake behaving animal subject. Engineering in Medicine and Biology Society, EMBC, 2011 Annual International Conference of the IEEE. Aug. 30 2011-Sept. 3 2011: pp.7658-7661.

[15] S Hao, J. Gorjon, S Taylor, SCIMITAR: subject-carried implant monitoring inductive telemetric ambulatory recorder for remote strain measurement on fracture fixation tibial nails. Medical Engineering and Physics, 2014, 36 (3): pp.405-411.